Zhang *et al. Chin. J. Mech. Eng.* (2021) 34:96
https://doi.org/10.1186/s10033-021-00614-y

Chinese Journal of Mechanical Engineering

ORIGINAL ARTICLE

Open Access

Subway Embedded Track Geometric Irregularity Safety Limits

Yuxiang Zhang[1], Jian Han[2*], Huilai Song[3] and Yu Liu[3]

Abstract

A coupling dynamic model of a subway train and an embedded track is established to study the safety limits of track irregularities. The simulated vehicle system was a 74-degrees of freedom multi-rigid body model, and the rail was a Timoshenko beam. The slab was a three-dimensional solid finite element model. The sensitive wavelength irregularity was first studied, and then the safety limit of the sensitive wavelength was analyzed. The wheel-rail lateral force exhibited a substantial effect on the track alignment and gauge irregularity safety limit. The wheel-rail vertical force and the rate of wheel load reduction significantly affected the height and cross-level irregularity safety limit. The results demonstrate that the safety limits of the alignment, gauge, height, and cross-level embedded track geometric irregularity are 5.3 mm, [− 10.5, 8] mm, 5.6 mm, and 6 mm, respectively.

Keywords: Embedded track, Irregularity, Sensitive wavelength, Safety limit

1 Introduction

With the rapid urbanization of China, an increasing number of cities have developed subways. Subways are favored by people due to their advantages such as fast speed, large traffic volume, and small space occupied. However, the vibration and noise generated by them can seriously affect the lives of residents near the lines [1–3]. To resolve this issue, embedded tracks are set on the slab rail groove, and rails are placed and set in the rail groove using a poured polymer elastic material. The continuous support of an embedded track can effectively reduce the vibration of the rail [4–6]; thus, embedded tracks can reduce ground vibration and noise. The geometric irregularity of a track is the primary source of wheel-rail vibration, and it directly affects the vehicle ride comfort and operation safety. The implementation of high ride comfort vehicles is one of the core challenges in the construction and maintenance of urban subway lines.

Oostermeijer et al. [7] used a computational model named "Rail" in 2000 to simulate the embedded track structure, considering the effect of continuous support by springs and damping units on beams. Markine et al. [8] established a coupling model for vertical high-speed vehicles and double-deck beam-embedded tracks in 2000. However, they did not consider three-dimensional (3D) coupling between the embedded tracks and trains. Ling et al. [9] established a coupling model for trams and embedded tracks. The model adopted multiple rigid bodies to simulate the vehicles, and the rail simulation was consistent with that of a traditional track. Deng et al. [10] used this model, based on the safety index limit, to analyze the limit of welded joint irregularity and analyze the tram-embedded track dynamic performance. Typical wheel/rail wear behavior in vehicle dynamics was also studied, and the corresponding embedded track structure parameters were optimized [11]. Han et al. [12–14] modeled the dynamic characteristics of a subway train-embedded track system; however, they did not research the geometric irregularities of the track.

At present, Chinese railways practice track irregularity peak and average management, and there are static and dynamic geometric smoothness control standards for non-ballast and ballast tracks for both newly built and rebuilt railways [15]. However, there is no control

*Correspondence: hanjian@swjtu.edu.cn
[2] School of Mechanical Engineering, Southwest Jiaotong University, Chengdu 610031, China
Full list of author information is available at the end of the article

standard for irregularities of an embedded track with continuous support in subway operating environments. In addition, current track geometric irregularity control standards seldom consider the influence of the track irregularity wavelength on the dynamic response of railway vehicles. Track irregularity is a random process that varies with mileage for wavelength components, ranging from a few millimeters to several hundred meters. Certain track irregularity wavelengths greatly influence the running quality of vehicles, while others do not. Therefore, it is necessary to strengthen the management of the embedded track geometry state to ensure sufficient smoothness of subway trains.

Therefore, railway operations must clarify the wavelength of railway line management and the range of sensitive wavelengths of railway track irregularities. Additionally, the relationship between the change in the wavelength of railway geometric irregularities and the dynamic response of railway vehicles is critical to the formulation of a railway track detection scheme and the analysis of detection data. Based on the subway vehicle-embedded track coupling dynamic model, this study presents an irregularity control strategy for an embedded track structure from two aspects: the track geometric irregularity sensitive wavelength and safety limit.

2 Methods

Based on the coupling dynamic analysis model of subway vehicle-embedded tracks and the irregularity input mode in Sections 2.1 and 2.2, respectively, the sensitive wavelength of the embedded track structure geometry irregularity was analyzed. Four basic geometric irregularity wavelengths of the alignment, gauge, height, and cross-level were assessed, and the correlation of the dynamic performance of subway vehicles was analyzed.

The range of random irregular track wavelengths is wide and can be sorted into short, medium, and long waves. Track geometric irregularities with a wavelength of less than 1 m are short-wave irregularities, which exhibit a high vibration frequency and significantly affect the wheel-rail noise, with little effect on the carriage body vibration and ride comfort. The medium wave irregularity wavelength ranges from 1 m to 30 m, and it primarily affects the safety and ride comfort of the vehicle. The wavelength of the long-wave irregularity is between 30 m and 200 m, which exhibits a critical effect on speed improvement and vehicle running comfort. The most crucial influence on the dynamic performance of a subway train is the medium wave irregularity, whose wavelength is less than 30 m, because the predominant running speed of a subway train is 50–90 km/h, and the length of a single vehicle is less than 30 m.

The irregularity limit was calculated based on the proposed dynamic performance index and sensitive wavelengths corresponding to the four irregularities. Two typical operational conditions were considered: the speed was set to 70 km/h in straight track line working conditions, and the speed was set to 50 km/h in the curve track line conditions, considering the small radius ($R=300$ m) curve of the actual subway line, and the superelevation was 100 mm.

2.1 Subway Vehicle-embedded Track Coupling Dynamic Model

The subway vehicle-embedded track coupling dynamic model (as displayed in Figure 1) consists of vehicle, track, and vehicle-track coupling excitation models.

2.1.1 Vehicle System

In this study, subway vehicle Type B was selected as the research object, and the vehicle system was simulated in a multi-rigid system model composed of a car body, bogie frames, rotary arms, wheelsets, and suspension systems. Three dynamic model views are presented in Figure 2. The wheelset and bogie frame are connected by a primary suspension, and the car body and bogie frame are connected by a secondary suspension. The secondary suspension model of the bogie includes 3D stiffness and damping, which are provided by the air spring, lateral bump stop of the secondary suspension of the rubber block, and vertical damper. The axle box suspension model includes 3D stiffnesses provided by the axle box spiral spring and elastic joints of the rotary arm. Primary vertical damping was provided by the primary vertical damper suspended outside of the axle box spring.

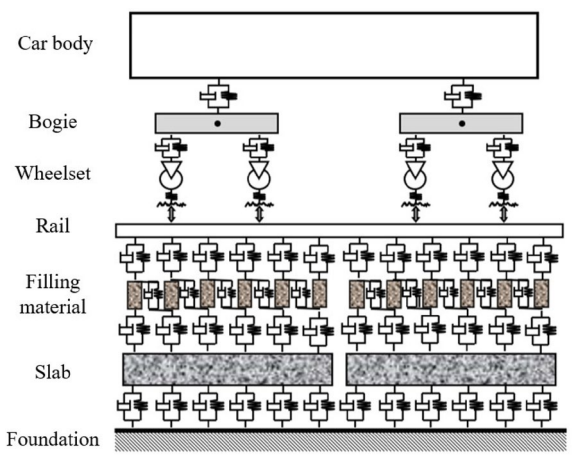

Figure 1 Schematic of embedded track dynamic model

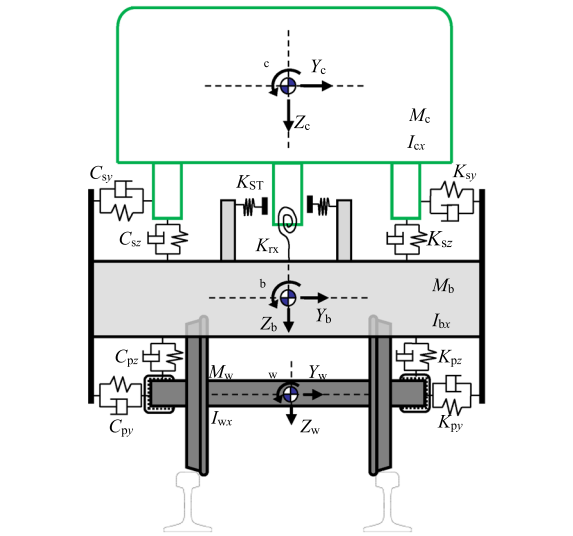

(a) Main view

(b) Side view

(c) Top view

Figure 2 Three views of subway vehicle dynamic model

Each car body, bogie, and wheelset consider six degrees of freedom (DOF) in the longitudinal, lateral, vertical, rolling, pitch (rotating), and yaw directions, and each rotary arm considers four DOF in the longitudinal, lateral, vertical, and pitch directions. The entire vehicle system contains a total of 74 DOF, as presented in Table 1.

The elastic deformations of all components of the vehicle system, such as the body, frame, and wheelset, were not considered. It was assumed that the wheelset only rolls when running on the rail, and no longitudinal slip occurs between the wheelset and rail. The nonlinear characteristics of the first and second suspension systems, such as the damping nonlinearity of the vertical damper, stiffness nonlinearity of the vertical bump stop of the primary suspension, and lateral bump stop of the secondary suspension, are considered.

According to the D'Alembert principle, the force analysis of each component of the subway vehicle system can be measured to obtain the interaction force between each component of the vehicle system; thus, the motion differential equation of each component of the vehicle system [16] is established.

2.1.2 Track System

The embedded track is considered to be composed of a rail, rail bearing groove filling material, slab, and foundation, as illustrated in Figure 3. Considering the vertical, lateral, and torsional vibrations of the rail, the left and right rails are treated as continuous elastic supports based on the Timoshenko beams. The slab was simulated using a 3D solid finite element, and the filling material for the bearing rail groove was simulated using a 3D viscoelastic spring-damper unit simulation, with its mass considered. The slab was connected to the foundation by spring/damping units that were equivalent to the stiffness of the foundation support.

2.1.3 Vehicle-track Coupling System

The vehicle and track systems interact with each other and are linked together. The vehicle-track coupling system must consider the wheel-rail spatial contact relationship and vehicle-track coupling interface excitation

Table 1 Subway Vehicle System DOF

Vehicle parts	DOF					
	Longitudinal	Lateral	Vertical	Rolling	Rotating/Pitch	Yaw
Wheelset ($i=1,4$)	X_{wi}	Y_{wi}	Z_{wi}	ϕ_{wi}	β_{wi}	ψ_{wi}
Left rotary arm ($i=1,4$)	X_{abLi}	Y_{abLi}	Z_{abLi}	–	β_{abLi}	–
Right rotary arm ($i=1,4$)	X_{abRi}	Y_{abRi}	Z_{abRi}	–	β_{abRi}	–
Bogie frame ($i=1,2$)	X_{bi}	Y_{bi}	Z_{bi}	ϕ_{bi}	β_{bi}	ψ_{bi}
Car body	X_c	Y_c	Z_c	ϕ_c	β_c	ψ_c

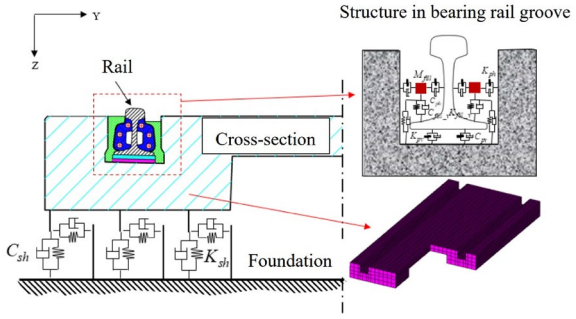

Figure 3 Schematic of embedded track dynamic model

mode. The wheel-rail spatially dynamic contact geometric relationship solution refers to the new wheel-rail spatially dynamic coupling model was proposed in Ref. [17]. The Hertz nonlinear elastic contact theory was adopted to solve the calculation of the wheel-rail normal force [18]. To calculate the wheel-rail creep force, the Kalker linear creep theory was first used [19]. After the creep between the wheel and rail reached saturation, the Shen-Hedrick-Elkins theory was applied for nonlinear correction [20]. The vehicle-track coupling excitation model adopts the "tracking window" model proposed in Refs. [21–23].

2.2 Track Geometry Irregularity Input Mode

Track geometry irregularities refer to deviations between the geometric dimensions of two rails relative to their ideal smooth states. Common track geometric irregularities predominately include four basic forms, alignment, height, gauge, and cross-level irregularities, as illustrated in Figure 4.

The displacement function can be used as the system excitation input of the vehicle-track coupling system, and the wheel-rail excitation caused by various track irregularities can be described by applying single harmonic irregularities in the same or opposite direction either in the same phase or out-of-phase using one or two rails.

3 Results

3.1 Analysis of Sensitive Wavelength of Geometric Irregularities

3.1.1 Alignment Irregularity

Alignment irregularity primarily causes the vehicle swing and shaking vibrations, increases the vehicle hunting motion and rolling swing motion, and results in a greater wheel-rail lateral force, rail tipping, and shifting of the track panel. The alignment irregularity of the continuously welded rail track also causes rail buckling, reducing operation safety. The investigation results demonstrate that the wheel-rail lateral force and derailment coefficient are most sensitive to alignment irregularity. Figure 5 illustrates the influence of the alignment irregularity

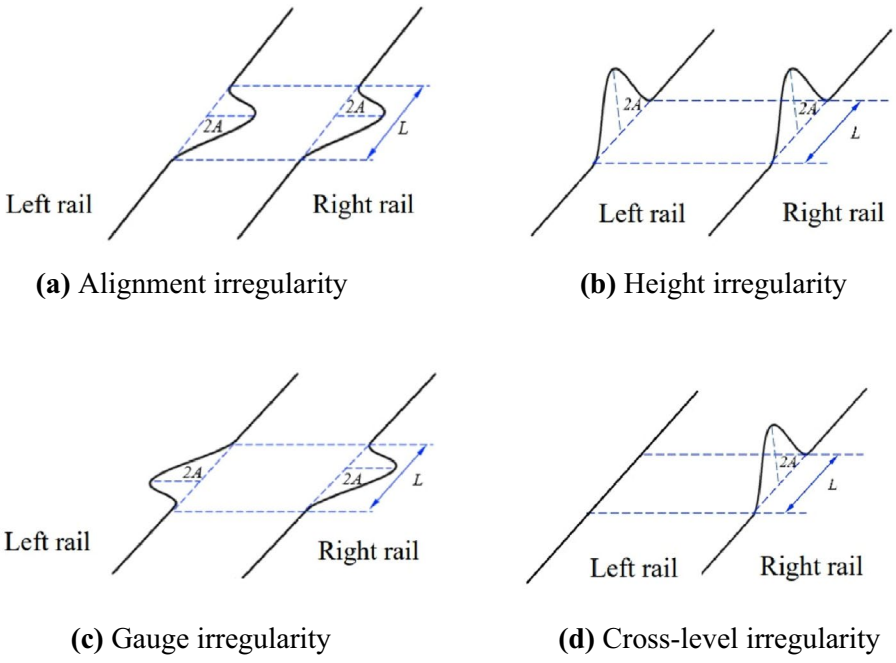

Figure 4 Types of irregularities. *L* is wavelength, and *A* is amplitude

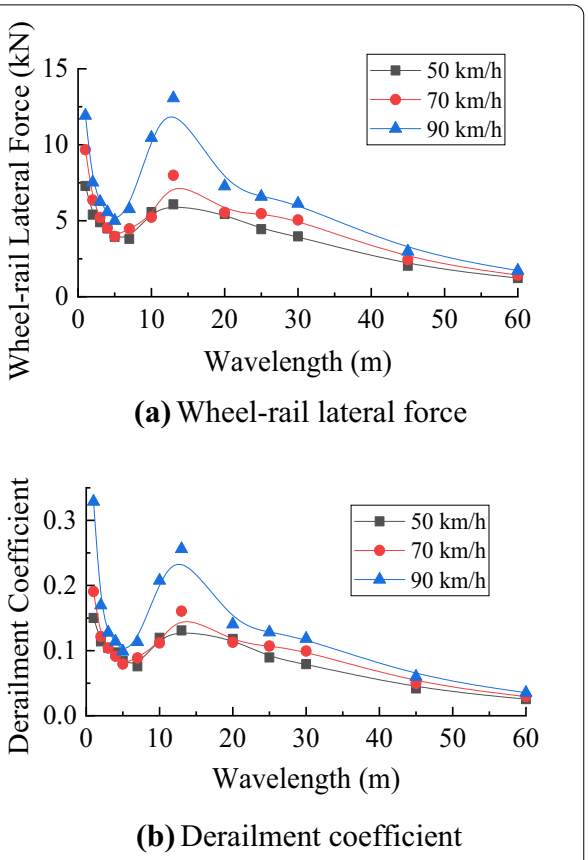

Figure 5 Influence of 10 mm alignment irregularity wavelength amplitude on derailment coefficient and wheel-rail lateral force

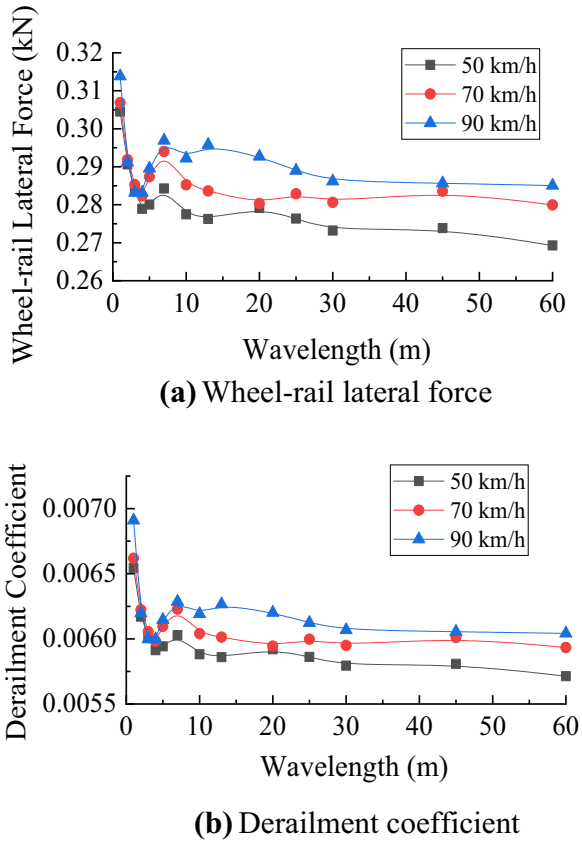

Figure 6 Influence of 10 mm gauge irregularity wavelength amplitude on derailment coefficient and wheel-rail lateral force

wavelength on the wheel-rail lateral force and derailment coefficient at speeds of 50 km/h, 70 km/h, and 90 km/h under an alignment irregularity amplitude of 10 mm.

From Figure 5, the wheel-rail lateral force and derailment coefficient are significantly nonlinear with a change in the wavelength of alignment irregularity, and their sensitive wavelengths range from 1 m to 5 m and 10 m to 20 m, respectively. Moreover, a local peak value appears at approximately 13 m. The wheel-rail lateral force and derailment coefficient increase with increasing speed and exhibit similar change trends.

3.1.2 Gauge Irregularity

Gauge irregularity may cause vehicle swing and yaw vibrations, increase the vehicle snaking and swing motions, and result in greater wheel-rail lateral force, rail tipping, and a shift in the track panel. That the wheel-rail lateral force and derailment coefficient are the most sensitive parameters to gauge irregularity. Figure 6 illustrates the influence of the gauge irregularity wavelength on the wheel-rail lateral force and derailment coefficient at speeds of 50 km/h, 70 km/h, and 90 km/h under an alignment irregularity amplitude of 10 mm.

From Figure 6, the wheel-rail lateral force and derailment coefficient decrease nonlinearly with an increase in the irregularity wavelength, particularly in the wavelength range of 1 m to 5 m. The gauge irregularity minimally affects the dynamic performance of subway vehicles when the wavelength is longer than 5 m. The wheel-rail lateral force and derailment coefficient increase with increasing speed and exhibit similar change trends.

3.1.3 Height Irregularity

The track height irregularity stimulates the pitch and vertical vibrations of the vehicle and causes wheel weight fluctuations, increases the wheel-rail vertical force, and increases the vertical acceleration of the vehicle body. It also affects the ride comfort of the continuously welded rail track and reduces the ride comfort and vehicle operation safety. The investigation results demonstrate that the wheel-rail vertical force and vertical ride comfort index are the most sensitive parameters to height irregularity

among the dynamic responses. Figure 7 displays the influence of the height irregularity wavelength on the wheel-rail vertical force and vertical ride comfort at driving speeds of 50 km/h, 70 km/h, and 90 km/h under a height irregularity amplitude of 10 mm.

From Figure 7, the vertical force and the vertical ride comfort of the wheel-rail are nonlinear with a change in the height irregularity wavelength. The sensitive wavelength range of the vertical force of the wheel and rail was 1–5 m. The sensitive wavelength corresponding to the vertical ride comfort index of the vehicle body ranges from 1 m to 20 m, and a local peak appears in the range of 5–13 m. These two indices increase with increasing speed and exhibit similar change trends.

3.1.4 Cross-level Irregularity

The track cross-level irregularity is derived from the height irregularity, which causes vehicle rolling vibrations, leads to an increase in the rate of wheel load reduction, increases the risk of derailment, and reduces operation safety. The investigation results illustrate that the rate of wheel load reduction and derailment coefficient are the most sensitive parameters to height irregularity. Figure 8 displays the influence of the cross-level irregularity wavelength on the rate of wheel load reduction and derailment coefficient at speeds of 50 km/h, 70 km/h, and 90 km/h under a cross-level irregularity amplitude of 10 mm.

It can be seen from Figure 8 that the rate of wheel load reduction and derailment coefficient exhibit a nonlinear decreasing trend with the change in the cross-level irregularity wavelength, and the sensitive wavelength ranges from 1 m to 10 m. These two indices increase with increasing speed and demonstrate similar change trends.

3.2 Control Limit Analysis of Rail Track Geometric Irregularity

3.2.1 Alignment Irregularity

The sensitive wavelength irregularity ranges are 1–5 m and 10–20 m, as described in Section 3.1.1. Hence, we selected an alignment irregularity wavelength of 1–2 m and an amplitude of 3–10 mm. Figure 9 displays the

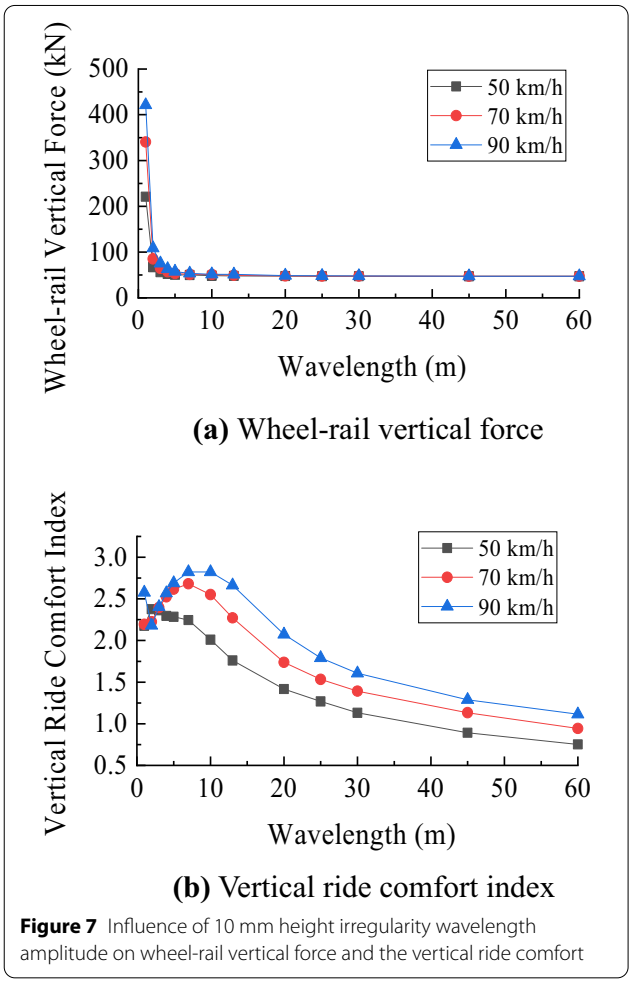

Figure 7 Influence of 10 mm height irregularity wavelength amplitude on wheel-rail vertical force and the vertical ride comfort

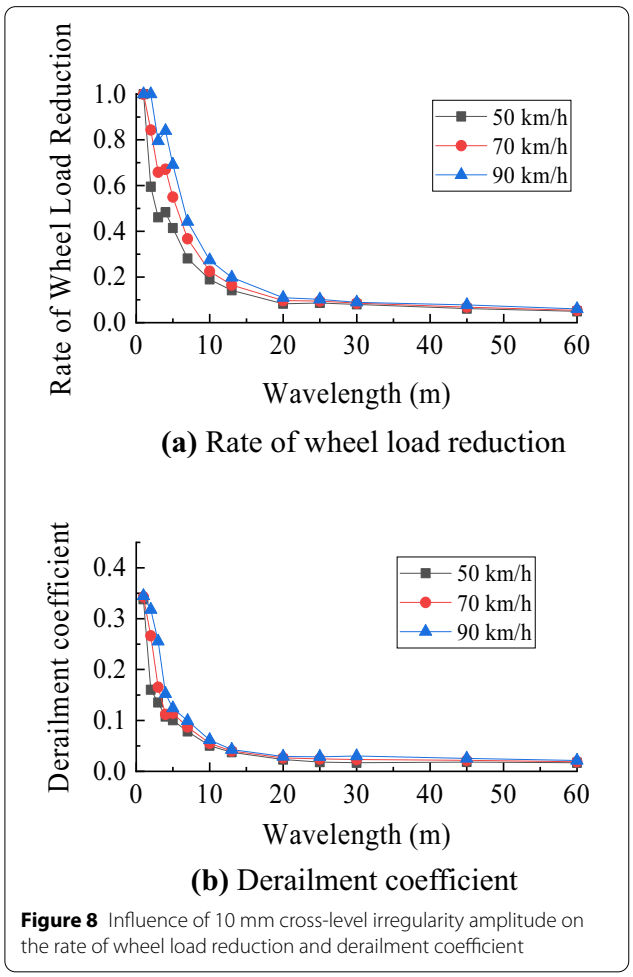

Figure 8 Influence of 10 mm cross-level irregularity amplitude on the rate of wheel load reduction and derailment coefficient

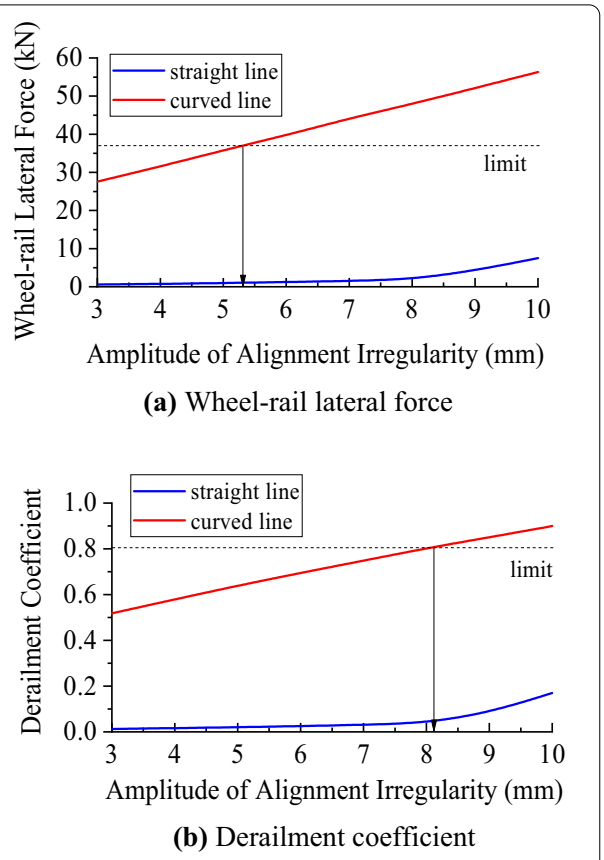

Figure 9 Influence of variation in alignment irregularity amplitude on wheel-rail lateral force and derailment coefficient under straight and curved operational line conditions

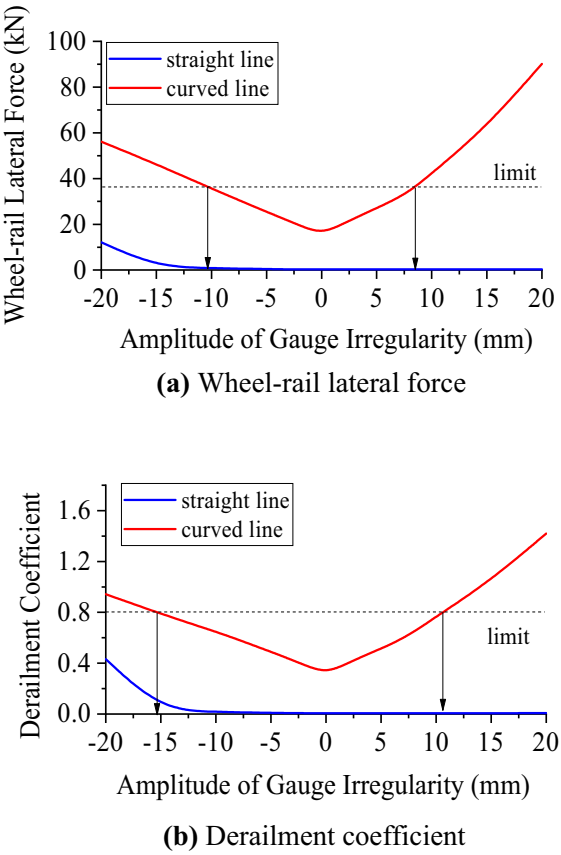

Figure 10 Influence of variation in gauge irregularity amplitude on wheel-rail lateral force and derailment coefficient under straight and curved operational line conditions

influence of the alignment irregularity amplitude on the wheel-rail lateral force and derailment coefficient under straight and curved operational line conditions.

From Figure 9, the dynamic response index of subway vehicles on the embedded track increases with an increase in the amplitude of the alignment irregularity. The irregularity limit as determined by the wheel-rail lateral force limit (36 kN) is approximately 5.3 mm, and the irregularity limit as determined by the derailment coefficient limit (0.8) is approximately 8.1 mm. Therefore, the wheel-rail lateral force is the key index for controlling the safety limit of the alignment irregularity. Considering a speed of 70 km/h in a straight line, a speed of 50 km/h in a curved line, and the highest alignment irregularity in the wavelength range, the safety limit of the embedded track alignment irregularity is set as 5.3 mm, which was determined according to the operational safety and ride comfort of subway vehicles on the embedded track.

3.2.2 Gauge Irregularity

The sensitive wavelength range of the gauge irregularity is 1–5 m, as described in Section 3.1.2. Hence, we selected a gauge irregularity wavelength of 1–2 m and an amplitude of 3–10 mm. Figure 10 illustrates the influence of the gauge irregularity amplitude on the wheel-rail lateral force and derailment coefficient under straight and curved operational line conditions.

From Figure 10, the wheel-rail lateral force and derailment coefficient increase symmetrically with the narrowing and widening of the gauge in the curved line; these two indices increase with the narrowing of the gauge, but they exhibit no changes with an increase in the gauge in the straight line. The safety limit for the gauge irregularity as determined by the wheel-rail lateral force limit (36 kN) is approximately [−10.5, 8] mm. The safety limit of the gauge irregularity determined by the derailment coefficient limit (0.8) is approximately [−15.5, 10.5] mm. Therefore, the wheel-rail lateral force is a vital

dynamic response index for controlling the safety limit of gauge irregularities. Considering a speed of 70 km/h in a straight line, a speed of 50 km/h in a curved line, and the highest gauge irregularity in the wavelength range, the safety limit of the embedded track gauge irregularity is set as [− 10.5, 8] mm, which was determined according to the operational safety and ride comfort of the subway vehicles on the embedded track.

3.2.3 Height Irregularity

The sensitive wavelength range of the height irregularity is 1–20 m according to Section 3.1.3. Hence, we selected a height irregularity wavelength of 1–2 m and an amplitude of 3–12 mm. Figure 11 displays the influence of the height irregularity amplitude on the wheel-rail vertical force and vertical comfort index under straight and curved operational line conditions.

From Figure 11, the dynamic response of the subway vehicle on the embedded track increases with an increase in the amplitude of the height irregularity. The safety limit for height irregularity as determined by the wheel-rail vertical force limit (135 kN) is approximately 5.6 mm. The safety limit of the height irregularity as determined by the vertical comfort index limit (2.5) is approximately 12 mm. Therefore, the wheel-rail vertical force is a vital dynamic response index for controlling the safety limit of the height irregularity. Considering a speed of 70 km/h in a straight line, a speed of 50 km/h in a curved line, and the highest height irregularity in the wavelength range, the safety limit of the embedded track height irregularity is set as 5.6 mm, which was determined according to the operational safety and ride comfort of the subway vehicles on the embedded track.

3.2.4 Cross-level Irregularity

The sensitive wavelength range of the height irregularity is 1–10 m according to Section 3.1.4. Hence, we selected a cross-level irregularity wavelength of 1–2 m and an amplitude of 3–12 mm. Figure 12 displays the influence of the cross-level irregularity amplitude on the rate of wheel load reduction and derailment coefficient under straight and curved operational line conditions.

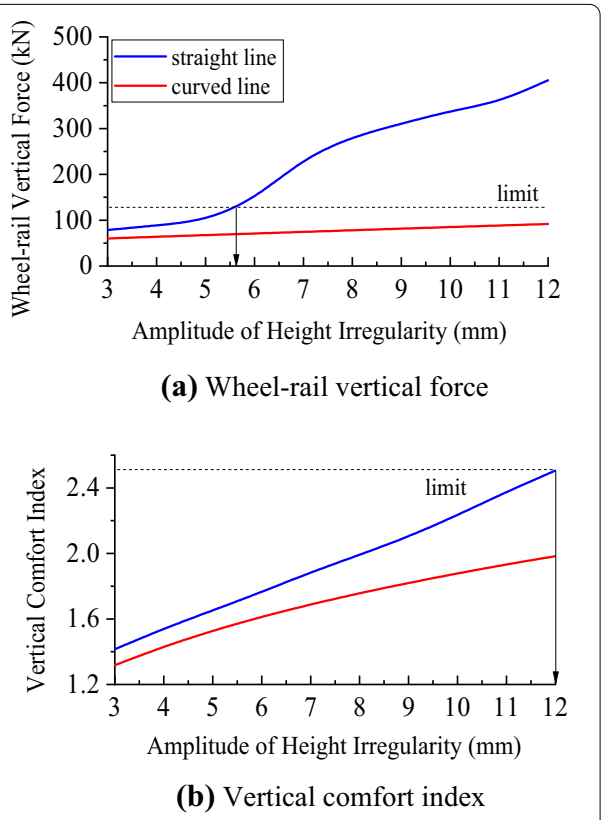

Figure 11 Influence of variation in height irregularity amplitude on wheel-rail vertical force and vertical comfort index under straight and curved operational line conditions

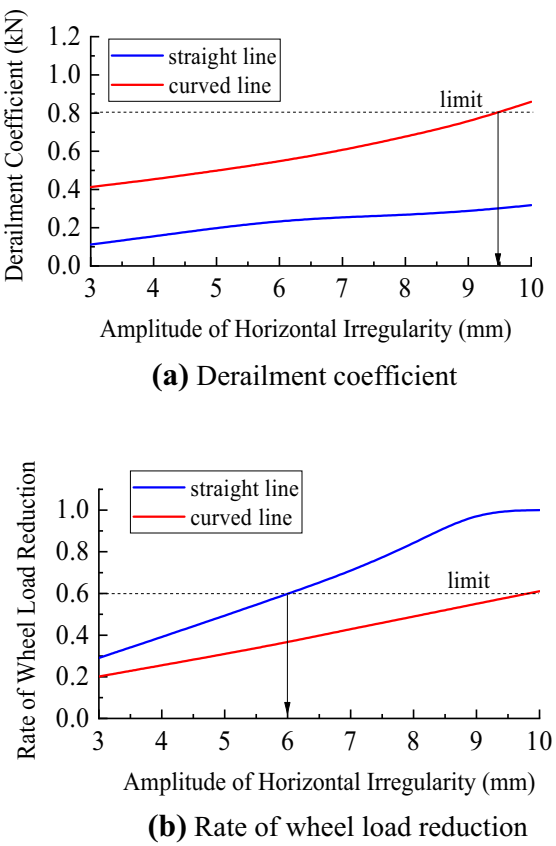

Figure 12 Influence of variation in cross-level irregularity wavelength amplitude on the rate of wheel load reduction and derailment coefficient under straight and curved operational line conditions

From Figure 12, the rate of wheel load reduction and the derailment coefficient of the subway vehicle on the embedded track increase with an increase in the amplitude of the cross-level irregularity. The safety limit for the cross-level irregularity as determined by the derailment coefficient limit (0.8) is approximately 9.5 mm. The safety limit of the cross-level irregularity as determined by the rate of wheel load reduction limit (0.6) is approximately 6 mm. Therefore, the rate of wheel load reduction is a critical dynamic response index for controlling the safety limit of cross-level irregularities. Considering a speed of 70 km/h in a straight line, a speed of 50 km/h in a curved line, and the highest cross-level irregularity in the wavelength range, the safety limit of the embedded track cross-level irregularity was set as 6 mm, which was determined per the operational safety and ride comfort of subway vehicles on the embedded track.

4 Conclusions

In this study, the sensitive wavelengths of four types of embedded track structure irregularities, i.e., alignment, gauge, height, and cross-level irregularities, were evaluated. The safety management limits of the geometric irregularities of the embedded track structures were systematically analyzed and discussed. The conclusions are as follows.

(1) A 74-DOF subway vehicle-embedded track coupling dynamic model was established to study the dynamic response of the vehicle and track.

(2) Different types of track geometric irregularities correspond to various vehicle response indices for sensitive wavelengths. The dynamic response indices dominating the safety limits of the alignment and gauge irregularities is the lateral wheel-rail force. The dynamic response indices dominating the safety limits of the height and cross-level irregularities are the vertical wheel-rail force, and the rate of wheel load reduction, respectively.

(3) Considering the operational speeds of 70 km/h for a straight line and 50 km/h for a small radius ($R = 300$ m) curved line, wheel-rail contact geometry, range of the most unfavorable irregularity wavelengths, and numerical calculation bias, the safety limits of the alignment, gauge, height, and cross-level irregularities were determined to be 5.3 mm, [−10.5, 8] mm, 5.6 mm, and 6 mm respectively, for optimal embedded track operational safety and comfort.

Acknowledgements
Not applicable.

Authors' Contributions
JH was in charge of the whole trial; YZ assisted with laboratory analyses; HS collected the data; YL assisted with sampling. All authors read and approved the final manuscript.

Authors' Information
Yuxiang Zhang, born in 1990, is currently a PhD candidate at *School of Economics and Management, Southwest Jiaotong University, China.*
Jian Han, born in 1987, is currently a research assistant at *School of Mechanical Engineering, Southwest Jiaotong University, China*. He received his PhD degree from *Southwest Jiaotong University, China*, in 2018. His research interests include the reduction of railway vibration and noise.
Huilai Song, born in 1994, is currently a PhD candidate at the *School of Civil Engineering, Southwest Jiaotong University, China.* He received his master degree from *Shijiazhuang Tiedao University, China*, in 2020. His research interests include track dynamics, and track structure maintenance theory & technology.
Yu Liu, born in 1982, is currently a lecturer at the *School of Civil Engineering, Southwest Jiaotong University, China*. He received his PhD degree from *Southwest Jiaotong University*, China, in 2013. His research interests include temperature field of slab track structure, track dynamics, and track structure maintenance theory & technology.

Funding
Supported by National Natural Science Foundation of China (Grant No. 51708459); Science and Technology Research and Development Program of China Railway (Grant No. N2019G037); and Sichuan Science and Technology Program (Grant No. 2020YJ0076).

Competing Interests
The authors declare no competing financial interests.

Author Details
[1]School of Economics and Management, Southwest Jiaotong University, Chengdu 610031, China. [2]School of Mechanical Engineering, Southwest Jiaotong University, Chengdu 610031, China. [3]School of Civil Engineering, Southwest Jiaotong University, Chengdu 610031, China.

Received: 10 February 2021 Revised: 3 August 2021 Accepted: 2 September 2021
Published online: 11 October 2021

References

[1] G X Chen, B Chen, X M Su, et al. Analysis and evaluation of ground vibration response induced by rapid rail transit. *Chinese Journal of Underground Space and Engineering*, 2008, 4(1): 27–34.
[2] Z Y Wang. *Field test and simulation analysis on environmental vibration of metro depot*. Nanchang: East China Jiaotong University, 2018.
[3] L Wei. *A study on the effect on environmental vibration induced by subway train*. Lanzhou: Lanzhou Jiaotong University, 2016.
[4] C Esveld. *Modern railway track (2nd Edition)*. Delft: Elsevier, 2001.
[5] C Esveld. Track structures in an urban environment. *Symposium K. U.*, Leuven, Belgium, 1997.
[6] S V Lier. The vibro-acoustic modelling of slab track with embedded rails. *Journal of Sound and Vibration*, 2000, 231(3): 805–817.
[7] K H Oostermeijer, A W M Kok. Dynamic behaviour of railway superstructures. *Heron*. 2000, 45(1): 25–34.
[8] V L Markine, A P Man, C Esveld. Optimization of an embedded rail structure using a numerical technique. *Heron*. 2000, 45(1): 63–74.
[9] L Ling, J Han, X B Xiao, et al. Dynamic behavior of an embedded rail track coupled with a tram vehicle. *Journal of Vibration and Control*, 2017, 23(14): 2355–2372.
[10] Y Q Deng, L Ling, X B Xiao, et al. On the safety criterion of welding irregularities on the embedded rail track. *Urban Mass Transit*, 2016, 5: 30–34, 39.
[11] Y Q Deng. *Study on dynamic interaction of tram train-embedded rail track*. Chengdu: Southwest Jiaotong University, 2014.
[12] J Han. *Study on dynamic behaviour and vib-acoustic characteristic of metro train and embedded track system*. Chengdu: Southwest Jiaotong University, 2018.
[13] J Han, Z H Li, X B Xiao, et al. Study on dynamic behaviour of metro train and embedded track system I: Theoretical modeling, experimental analysis and verification. *Journal of mechanical engineering*, 2020, 56(22): 148–158.

[14] J Han, X B Xiao, G Yang, et al. Study on dynamic behaviour of metro train and embedded track system II: Effect of track parameters on dynamic behaviour. *Journal of mechanical engineering*, 2020, 56(24): 173–180.
[15] TB10082-2005/J448-2005. *Standard for railway track design*. Ministry of Railways of China, Beijing: China Railway Publishing House, 2005.
[16] W M Zhai. *Vehicle-track Coupling Dynamics* (*Third edition*). Beijing: Science Press, 2007.
[17] G Chen, W M Zhai. A new wheel/rail spatially dynamic coupling model and its verification. *Vehicle System Dynamics*, 2004, 41(4): 301–322.
[18] X S Jin, Q Y Liu. *Tribology of wheel and rail*. Beijing: China Railway Publishing House, 2004.
[19] J J Kalker. *On the rolling contact of two elastic bodies in the presence of dry friction*. Netherland: Delft University, 1967.
[20] Z Y Shen, J K Hedrick, J A Elkins. A comparison of alternative creep force models for rail vehicle dynamic analysis. *Vehicle System Dynamics*, 1983, 12(1–3): 79–83.
[21] X B Xiao, X S Jin, Z F Wen, et al. Effect of tangent track buckle on vehicle derailment. *Multibody System Dynamics*, 2011, 25(1): 1–41.
[22] X B Xiao, L Ling, X S Jin. A study of the derailment mechanism of a high speed train due to an earthquake. *Vehicle System Dynamics*, 2012, 50(3): 449–470.
[23] X S Jin, X B Xiao, L Ling, et al. Study on safety boundary for high-speed train running in severe environments *International Journal of Rail Transportation*, 2013, 1(1–2): 87–108.